Journal of Inflammation Research

Dovepress
Taylor & Francis Group

Open Access Full Text Article

ORIGINAL RESEARCH

Analysis and Validation of Mitophagy-Related Genes in Diabetic Foot Ulcers

Shaoyihan Fang[1,*], Huijuan Zhang[1,*], Wenjian Liu[2,*], Shuangyan Li[3], Zhenzhen Chen[4], Jingjie Min[1], Chengyu Dai[1], Jingwen An[1], Hongxiao Zhang[1], Dewu Liu[1]

[1]Medical Center of Burn Plastic and Wound Repair, The First Affiliated Hospital, Jiangxi Medical College, Nanchang University, Nanchang, 330031, People's Republic of China; [2]Department of Burns and Plastics, Jiangxi Provincial Corps Hospital of Chinese People's Armed Police Forces, Nanchang, 330001, People's Republic of China; [3]Department of Critical Care Medicine, Ezhou Central Hospital, Ezhou, Hubei, 436000, People's Republic of China; [4]Outpatient Department, Jiangxi Provincial People's Hospital, The First Affiliated Hospital of Nanchang Medical College, Nanchang, Jiangxi, 330006, People's Republic of China

*These authors contributed equally to this work

Correspondence: Dewu Liu, Medical Center of Burn Plastic and Wound Repair, The First Affiliated Hospital, Jiangxi Medical College, Nanchang University, Nanchang, 330031, People's Republic of China, Email dewuliu@126.com

Purpose: This study aimed to identify hub genes associated with mitophagy involved in the pathogenesis and progression of diabetic foot ulcer (DFU), and to characterize their immune cell infiltration features and single-cell expression profiles.

Methods: DFU-related datasets (GSE80178, GSE68183) were retrieved from the GEO database. Subsequently, differentially expressed genes (DEGs) were identified via limma analysis, followed by gene set enrichment analysis (GSEA) to assess gene function enrichment. Identified DEGs were intersected with mitophagy-related genes. Machine learning (ML) algorithms were further employed to identify hub genes. Additionally, immune cell infiltration was examined via the CIBERSORT algorithm, and the correlation between the identified genes and immune infiltration was investigated. Finally, hub genes identified were validated via the single-cell RNA sequencing dataset GSE165816, and further validated using RT-PCR and Western blot (WB) assays.

Results: Two hub genes, ANO6 and ALDH2, were identified and found to be significantly downregulated in the skin tissues of patients with DFU. Receiver operating characteristic (ROC) analysis demonstrated robust diagnostic potential (ANO6, AUC = 0.833, ALDH2, AUC = 0.806). Immune cell infiltration analysis demonstrated notable differences between the DFU and normal groups in naïve B cells, monocytes, resting mast cells, γδT cells, and regulatory T cells (Tregs). The findings were further validated through single-cell RNA sequencing (scRNA-seq) analysis and experimental studies, which confirmed the downregulation of ANO6 and ALDH2 in DFU tissues.

Conclusion: Two mitophagy-related hub genes, ANO6 and ALDH2, were identified and validated as being significantly down-regulated in DFU. Both genes demonstrated diagnostic potential and showed an association with immune cell infiltration. These findings suggest that mitophagy dysfunction may contribute to the pathophysiology of DFU, potentially through the dysregulation of inflammatory pathways and immune responses. While the results provide valuable insights into DFU and its management, further studies with larger cohorts and deeper exploration of mechanistic links to inflammation are necessary to translate these findings into therapeutic strategies.

Keywords: DFU, mitophagy, single-cell RNA-seq, bioinformatics analysis

Introduction

Diabetic foot ulcer (DFU) is a leading cause of high amputation and mortality among patients with diabetes. It is characterized by damage to the epidermis or partial dermis of the foot.[1,2] Clinically, DFU is commonly classified into three types based on etiology: neuropathic ulcers, neuroischemic ulcers, and ischemic ulcers. It is estimated that over 550 million people worldwide have diabetes, and up to 34% of these patients will develop foot ulcers, with approximately 20% of DFU patients undergoing lower limb amputation. The recurrent nature of DFU imposes a significant economic burden on both patients and society,[3,4] therefore highlighting the urgent need to develop potential therapeutic targets and novel treatment strategies.

Received: 18 November 2024
Accepted: 11 March 2025
Published: 25 March 2025

Mitophagy is a selective form of cellular autophagy that transports damaged mitochondria to the lysosome for degradation, maintaining intracellular homeostasis.[5] When mitophagy dysfunction occurs, the dysfunctional and damaged mitochondria can release high levels of reactive oxygen species (ROS) that accumulate within the cell, leading to apoptosis.[6] The pathophysiology of wounds in DFU differs from that of normal wounds, characterized by an extended inflammatory phase, a limited proliferative phase, and a disordered remodeling phase.[7,8] Cells in the wound microenvironment are subjected to a series of harmful effects, including hyperglycemia, metabolic products of glucose, oxidative stress-induced ROS, and repeated local infections by pathogenic microorganisms.[9] These factors can trigger the release of a range of anti-inflammatory and pro-inflammatory cytokines.[5,10,11] Studies have shown that mitophagy dysfunction occurs in DFU, causing cellular homeostasis imbalance and exacerbating the inflammatory microenvironment of the wound.[12–14] Targeting mitophagy may provide a promising strategy for the diagnosis, treatment, or management of DFU. Therefore, investigating mitophagy-related genes associated with DFU is crucial for deepening our understanding of its pathogenesis, improving diagnostic and therapeutic approaches, and enhancing evaluations for prognosis.

This study adopted machine learning (ML) algorithms, specifically Support Vector Machine Recursive Feature Elimination (SVM-RFE) and Random Forest (RF), to identify differentially expressed genes (DEGs) through bioinformatics methodologies based on transcriptome sequencing. The diagnostic significance of hub genes was assessed through the construction of receiver operating characteristic (ROC) curves, and a nomogram was created to illustrate the relationships among hub genes within the predictive model. Further validation of the expression of hub genes was performed in various single-cell types using the single-cell RNA sequencing (scRNA-seq) dataset. RT-PCR and Western blot (WB) assays were performed to detect the expression of the identified mitophagy-related hub genes and their corresponding proteins in DFU tissues. This work expands the mitophagy-related gene research relevant to DFU, identifying ALDH2 and ANO6 as potential novel regulators of diabetic wound healing. These findings enhance our understanding of mitophagy's role in DFU progression and provide insights into its molecular mechanisms, diagnosis, and treatment.

Materials and Methods

Microarray Data Collection

RNA sequencing data were acquired from DFU and normal tissue samples (GSE80178, GSE68183) sourced from human subjects. The GSE80178 dataset comprised 3 normal tissue samples and 9 DFU tissue samples, whereas GSE68183 contained 3 normal skin tissue samples and 3 DFU tissue samples. scRNA-seq data from DFU tissues and normal tissue samples were obtained from the dataset GSE165816. All datasets were downloaded from the GEO (https://www.ncbi.nlm.nih.gov/geo/) database. Mitophagy-related genes were sourced from the GeneCards (https://www.genecards.org/) database.

DEG Identification and Functional Enrichment Analysis

We normalized the GSE80178 and GSE68183 datasets using the "normalize between arrays" function to eliminate batch effects between the two GEO datasets. The "limma" package was employed for differential expression analysis, with thresholds set at $P < 0.05$ and $|\log2(FC)| > 1$ to identify DEGs,[15] when $\log2(FC) > 1$, the DEG was considered upregulated in the DFU group compared to the normal group, while when the value < -1, it was considered downregulated. The R programs "ggplot2" and "pheatmap" were employed to respectively create volcano plots and heatmaps, to visualize the DEGs.[16] We performed gene ontology (GO) and Kyoto Encyclopedia of Genes (KEGG) analyses to investigate the probable biological processes linked to the DEGs[17] using the "clusterProfiler" package in R. Subsequently, gene set enrichment analysis (GSEA) was carried out utilizing the R package "ReactomePA". The results were visualized accordingly.[18]

Identification of Hub Genes

A Venn diagram displaying the differentially expressed mitophagy-related genes was created by intersecting DEGs with 271 mitophagy-related genes from the GeneCards database using the R package "VennDiagram". Two ML methods were employed to screen for hub genes in this study. First, the "e1071" package was adopted to perform SVM-RFE analysis.

The average misclassification rate was evaluated using 10-fold cross-validation, and the core feature genes that contributed most to the model's performance were selected. Next, the Random Forest (RF) algorithm was adopted to perform random sampling with replacement on the DEGs, ensuring the accuracy of results even in case of data loss. The overlapping biomarkers identified by both algorithms were considered the optimal mitophagy-related gene biomarkers for DFU. The "pROC" package in R was utilized to construct ROC curves, and the area under the ROC curve (AUC) was computed to assess the diagnostic significance of the hub genes.[19] When the DFU group and the normal group were mismatched or when there was a change in the sample distribution of the dataset, the ROC curve could stably assess the diagnostic performance of the model. A nomogram was ultimately developed with the "rms" package to visualize the relationships between hub genes within the predictive model.

Immune Infiltration Analysis

CIBERSORT (https://cibersortx.stanford.edu/) bioinformatics technique was employed to assess immune cell infiltration in order to examine the variations in the relative proportions of immune cells between DFU and normal tissues. A reference set comprised of 22 immune cell subtypes (LM22) with 1,000 permutations was used to compute the estimated relative abundance of immune cells. After that, to investigate how the immune cell infiltration of DFU and control samples differed, a bar plot was created via the "ggplot2" package. Additionally, the relationships between the identified hub genes and the 22 immune cell subtypes were also visualized.

scRNA-Seq Dataset Download and Processing

The scRNA-seq dataset GSE165816 was processed using the R package "Seurat", and 11 cases of normal skin tissue and 13 cases of foot skin tissue from DFU patients were selected from the dataset. Cell quality control was performed by evaluating the proportion of mitochondrial genes, the number of RNA features per single cell, and the total RNA sequencing count. Cells with mitochondrial genes accounting for less than 10% were retained, along with cells that had more than 200 genes, gene expressions ranging from 500 to 8000, and genes expressed in at least three cells. The LogNormalize function was adopted to normalize the expression level of each cell.[20] Principal component analysis (PCA) was performed for dimensionality reduction, and t-SNE was used for cell clustering and visualization with a resolution setting of 20. The FindMarkers function was utilized to identify cells marked by known cell surface-specific markers. Finally, the PercentageFeatureSet function was applied to import hub genes, to quantify the expression distribution of hub genes expressed within different cell types.

Patient Recruitment and Clinical Data Collection

From June 2024 to August 2024, five DFU patients were recruited from the Department of Burn Surgery, First Affiliated Hospital of Nanchang University, for the collection of ulcer tissue from the wound and normal skin tissue from the perilesional area or discarded normal skin tissue after skin graft surgery. Normal skin tissue samples were collected from five patients in the Department of Plastic Surgery at the same hospital, either from normal skin tissue adjacent to scars during scar excision surgeries or discarded normal skin tissue after skin graft surgery. The protocol of the present study was approved by the Ethics Committee, the First Affiliated Hospital of Nanchang University, and adhered to the Declaration of Helsinki. Participants of this study provided written informed consent before the study commenced.

RT-PCR and WB Validation of Target Gene Expression in Clinical Samples

The collected clinical tissue samples were ground to extract RNA with Trizol. After RNA concentration was measured using a NanoDrop One UV-Vis spectrophotometer (Thermo Fisher Scientific, USA), RNA was reverse transcribed into cDNA according to the instructions of the TransScript One-Step gDNA Removal and cDNA Synthesis SuperMix kit (TransGen Biotech, China) using the Applied Biosystems 2720 Thermal Cycler (Thermo Fisher Scientific, USA). Primer synthesis services were provided by Sangon Biotech. Real-time PCR was employed using the ABI StepOne Plus™ Real-Time PCR System with the 2× M5 hiPer Realtime PCR SuperMix (Mei5bio, China). Relative expression levels of RNA were determined via the $2^{-\Delta\Delta CT}$ method, with experiments performed in triplicate.

Tissue proteins were extracted using the RIPA method. The primary antibodies used were rabbit-derived anti-human ANO6 (Abmart, Shanghai, China) and anti-ALDH2 (Abclonal, Wuhan, China), along with the internal control antibody GAPDH (Proteintech, Wuhan, China). The secondary antibody was goat anti-rabbit (Abclonal, Wuhan, China). All antibodies were diluted according to the manufacturer's instructions. The 10% PAGE gel was prepared using a PAGE Gel Fast Preparation Kit (Epizyme, Shanghai, China) according to the instructions. The electrophoresis buffer and transfer buffer were prepared using Fast Electrophoresis Powder and Fast Transfer Powder (Servicebio, Wuhan, China) as per the instructions. Western blot experiment was conducted using a vertical electrophoresis system (Bio-Rad, USA).

Primer sequences are as follows, with β-actin serving as the internal control.

Primer sequences for ANO6: F: TACCTGACTCCACAGACAGCCA, R: ATCAGTCTGGGTCCTTGGGAGT.

Primer sequences for ALDH2: F: TTGCCTCCCATGAGGATGTGGA, R: TTGCCTCCCATGAGGATGTGGA.

Primer sequences for β-actin: F: TCTCCCAAGTCCACACAGG, R: GGCACGAAGGCTCATCA.

Statistical Analysis

Bioinformatics and statistical analyses were performed utilizing R (version 4.4.0). Quantitative results were evaluated using Prism v9.0 and presented as mean ± standard deviation (SD). The *t*-test was adopted to appraise group differences, with $P < 0.05$ denoting statistical significance.

Results

Identification of DEGs Between DFU and Normal Samples

The GSE80178 and GSE68183 datasets were integrated to eliminate batch effects and normalized (Figure 1A and B). A 2D principal component analysis (PCA) clustering plot demonstrated the differences between the two groups after integration (Figure 1C). Based on differential expression analysis, 857 DEGs were identified in the DFU group ($|\log2(FC)| > 1$, $P < 0.05$), including 269 genes upregulated and 588 genes downregulated. The DEGs were visualized via volcano plot and heatmap (Figure 1D and E).

Functional Enrichment Analysis of DEGs

In order to investigate the potential biological processes related to DFU, pathway enrichment analysis was performed on identified DEGs. The GO analysis, including biological process (BP), cellular component (CC), and molecular function (MF), then revealed enrichment in pathways such as skin epidermal and dermal development, extracellular matrix structure, regulation of monocyte chemotaxis involved in immune response, lysosomal lumen, basement membrane, centrosome satellite, glutathione peroxidase activity, proteoglycan binding, and cell resistance to stress (Figure 2A). KEGG analysis revealed that the DEGs were functionally enriched in pathways related to cytokine-receptor interactions, amino acid metabolism, and fatty acid metabolism (Figure 2B). GSEA results showed that two mitophagy-related pathways, Lysosome and Phagosome, were downregulated in DFU (Figure 2C), suggesting potential mitophagy dysfunction in DFU. Subsequently, 271 mitophagy-related genes were retrieved from the GeneCards database, and 10 mitophagy-related DEGs were identified, including MAP1LC3A, BNIP3, TIGAR, HK2, RHOT1, VPS13C, ALDH2, ARL6IP5, ANO6, and BCL2 (Figure 2D).

Identification of Hub Genes

To further identify hub genes, this study employed SVM-RFE and RF algorithms. Through SVM-RFE, two genes were identified as candidate hub genes (Figure 3A). Feature importance was determined using the RF algorithm, and genes with an importance score greater than 1 were selected as candidate hub genes (Figure 3B and C). The common candidate genes identified by both methods were deemed as the hub genes for this study, specifically ANO6 and ALDH2. The ROC curve results demonstrated that the AUC values for both hub genes were higher than 0.7, indicating their diagnostic value. Subsequently, ROC curves were constructed for hub genes. The results indicated that both hub genes had AUC values above 0.7, suggesting favorable diagnostic performance for DFU (ANO6, AUC = 0.833; ALDH2, AUC = 0.806) (Figure 3D and E). A nomogram was also plotted to visualize the relationship between ALDH2 and ANO6 in the predictive model, as well as the morbidity. The calibration curve demonstrated the accuracy of the model's predictions (Figure 3F).

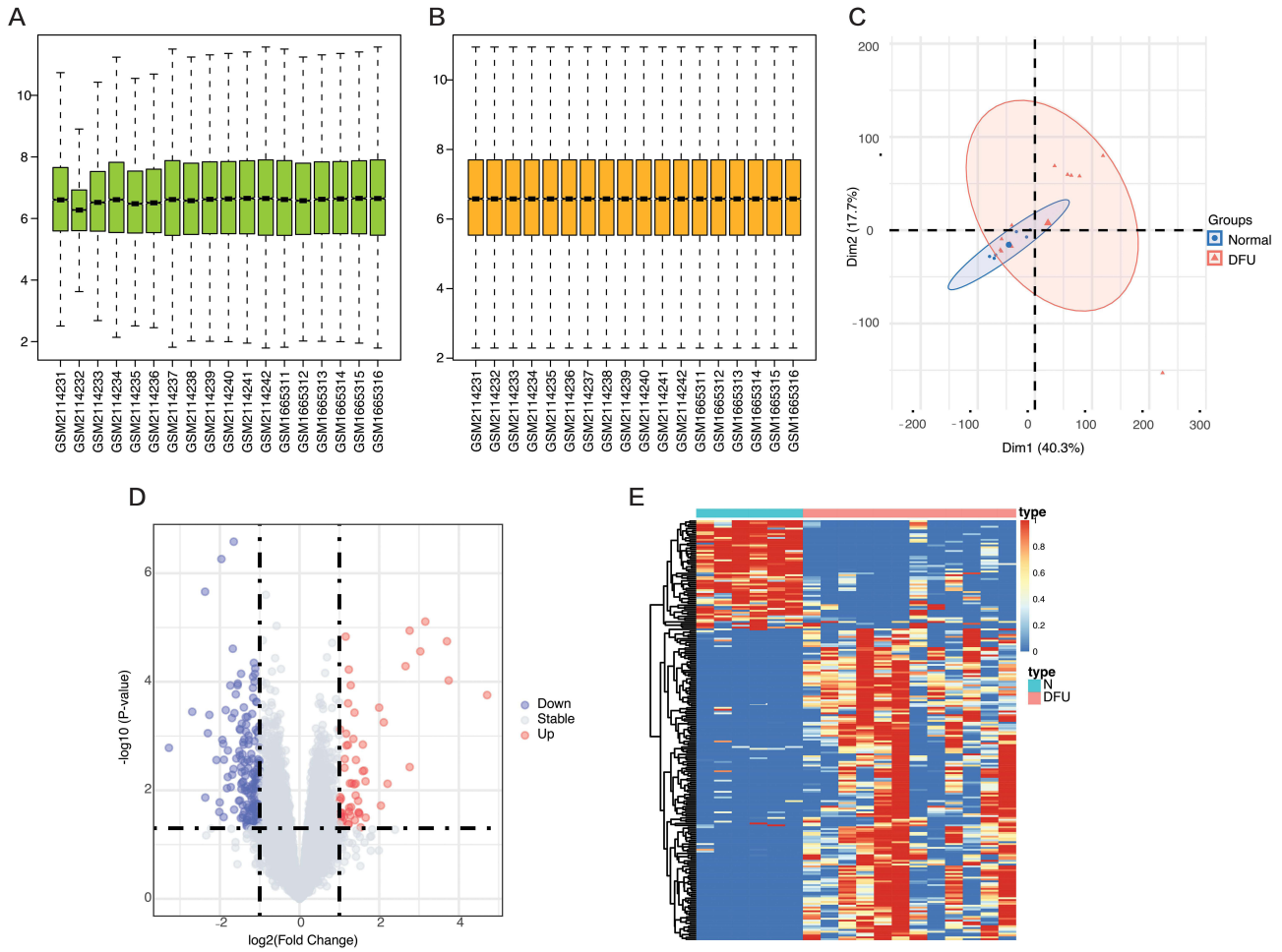

Figure 1 DEG identification between normal and DFU groups. (**A**) Boxplot of the integrated GSE80178 and GSE68183 datasets; (**B**) Boxplot after normalization; (**C**) PCA clustering plot of normal and DFU groups; (**D**) Volcano plot of DEGs in normal and DFU groups; (**E**) Heatmap of DEGs in normal and DFU groups.

Immune Cell Infiltration and Correlation Analysis

The CIBERSORT algorithm was utilized to determine the relative proportions of 22 immune cell types in the samples (Figure 4A). Compared to normal subjects, the DFU samples exhibited increased infiltration of naïve B cells and monocytes, while infiltration of resting mast cells, γδT cells, and Tregs was decreased (Figure 4B). Correlation analysis indicated that the ALDH2 gene had a positive correlation with follicular helper T cells and resting mast cells, while demonstrating a negative correlation with resting NK cells, monocytes, and eosinophils (Figure 4C). The ANO6 gene had a positive correlation with γδT cells, resting mast cells, and M1 macrophages, and it demonstrated a negative correlation with plasma B cells, monocytes, and naïve B cells (Figure 4D).

Validation of Hub Genes at the scRNA-Seq Level

With the t-SNE clustering algorithm, all cells were clustered into 21 categories (Figure 5A). Based on the expression of established cell-specific marker genes, 10 cell types were identified: mesenchymal stem cells, fibroblasts, keratinocytes, T cells, chondrocytes, monocytes, endothelial cells, astrocytes, B cells, and NK cells (Figure 5B). To evaluate the variations in hub gene expression among cell types, the PercentageFeatureSet function was employed to input the identified mitophagy-related hub genes ALDH2 and ANO6, and the percentage of each hub gene in every cell type was obtained. Data from foot skin samples of 10 healthy individuals and 14 DFU patients were analyzed. The results showed that ALDH2 was relatively highly enriched in keratinocytes, while ANO6 was enriched in fibroblasts (Figure 5C-E). Compared to the normal group, the expression levels of ALDH2 and ANO6 were both decreased in the DFU group (Figure 5F).

https://doi.org/10.2147/JIR.S504001

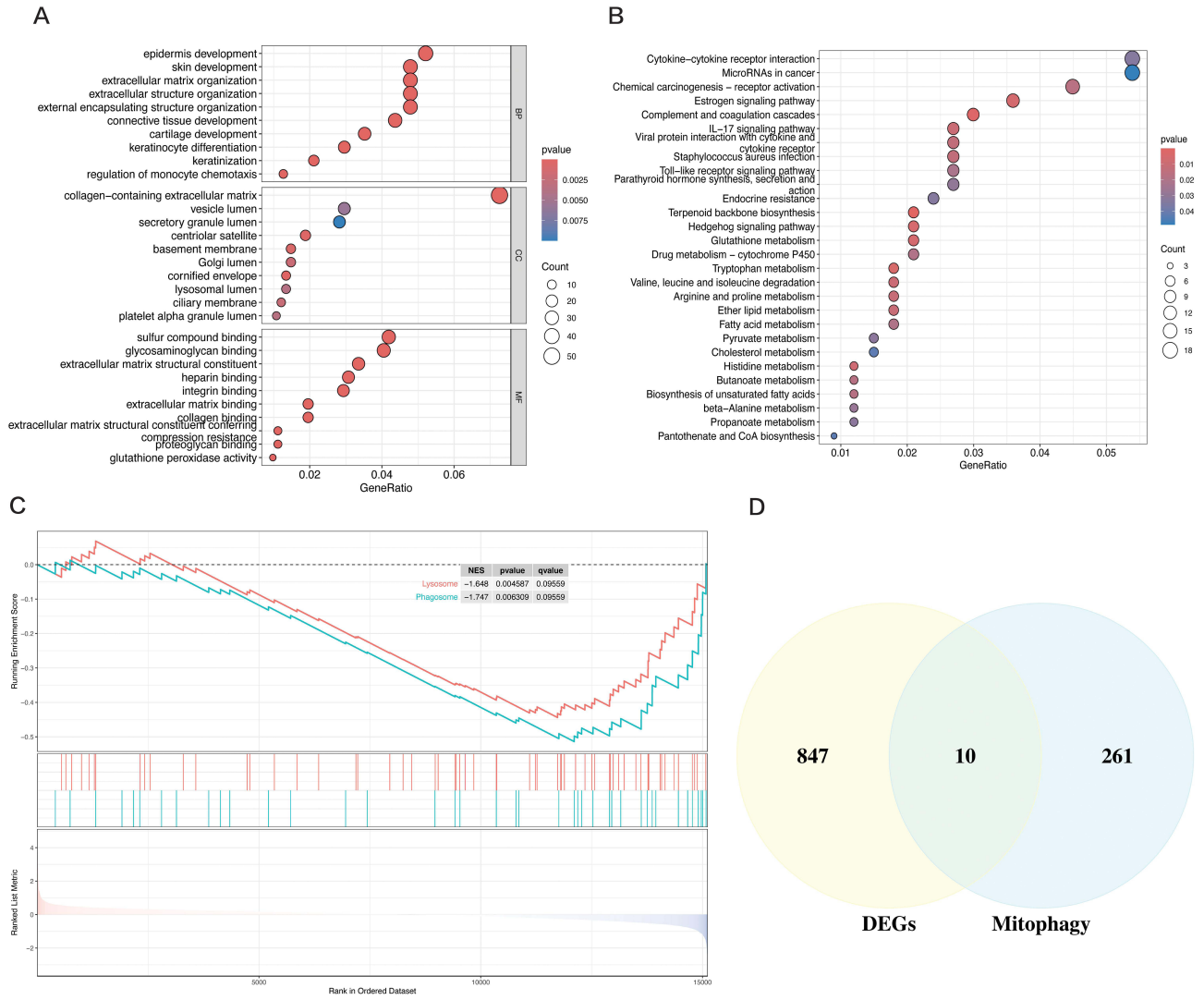

Figure 2 DFU-related DEGs - functional enrichment analysis. (**A**) GO analysis of DEGs; (**B**) KEGG analysis of DEGs; (**C**) GSEA of mitophagy-related DEGs; (**D**) Venn diagram of mitophagy-related DEGs.

Validation of hub gene expression levels in clinical tissues

The Expression Levels of the Two Hub Genes, ANO6 and ALDH2, in the normal and DFU groups are shown in Figure 6A and B. In the GSE80178 and GSE68183 datasets, ANO6 and ALDH2 were found to be expressed at lower levels in the DFU group, with gene expression patterns consistent with the results from single-cell analysis. To further validate these findings, RT-PCR and Wb assays were performed on skin tissue samples from both the normal and DFU groups for confirmation of the expression levels of the hub genes and their proteins. The results showed that both ANO6 and ALDH2 were significantly downregulated at the RNA and protein levels in the DFU group compared to the normal group (Figure 6C–G).

Discussion

In recent decades, substantial efforts have been dedicated to exploring the pathophysiology of cells in DFU tissues, significantly enhancing our understanding of the wound-healing process of this disease. Increasing evidence has suggested that mitophagy phenotypes are associated with the wound-healing process in DFU. In this study, we retrieved data from the GEO database, including two previously published datasets, GSE68183 (whole-genome mRNA microarray) and GSE80178, which provide information on mRNA expressions in DFU tissues. Additionally, the inclusion of

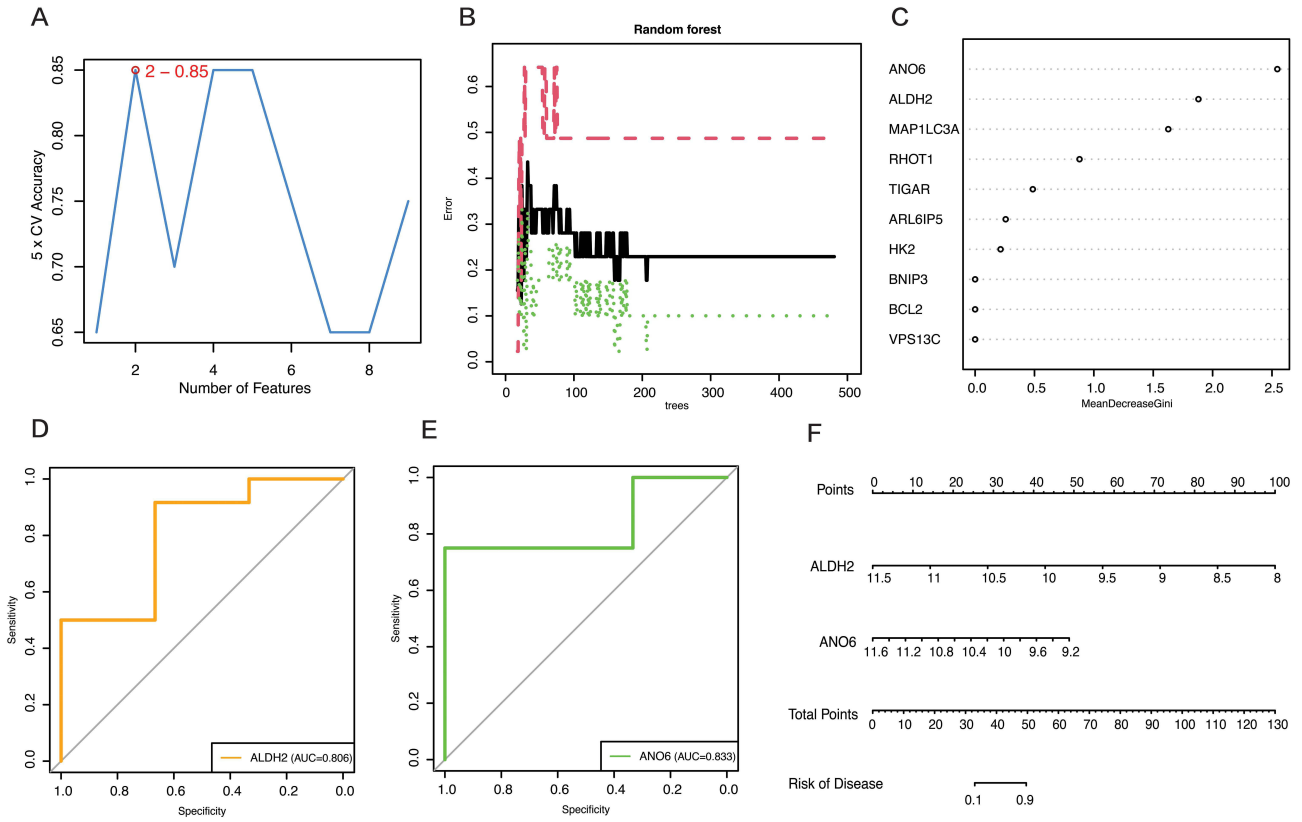

Figure 3 Hub gene identification. (**A**) SVM-RFE analysis of hub genes; (**B** and **C**) RF analysis of hub genes; (**D** and **E**) ROC curves of hub genes; (**F**) Nomogram of hub genes.

the scRNA-seq dataset GSE165816 yielded valuable information regarding the molecular pathogenesis and pathophysiology of immune responses and mitophagy in DFU.

Mitophagy has been widely studied in various human diseases, including neurodegenerative diseases, cardiovascular diseases, pulmonary diseases, acute kidney injury, alcoholic liver disease, skeletal muscle aging, cancer, autoimmune diseases, and metabolic syndrome. Mitophagy dysfunction plays a crucial role in the pathogenesis of diabetes-related complications, such as diabetic cardiomyopathy and diabetic nephropathy. Mitochondria are dynamic organelles that supply energy essential for cell survival.[21] Under normal conditions, a dynamic balance is maintained between mitochondrial fusion and fission,[22,23] when this balance is disrupted, pathological conditions of excessive or insufficient mitophagy occur, leading to disease onset. Increasing evidence suggests that, mitophagy is involved in many biological processes, including inflammation, metabolic transformation, and cellular reprogramming.[24] Research has shown that hyperglycemia is directly linked to mitochondrial oxidative stress. Hyperglycemia can induce mitochondrial dysfunction, resulting in increased mitochondrial ROS release, decreased ATP production, and mitochondrial membrane depolarization, which collectively impair mitochondrial homeostasis.[12,25–27] Mitophagy is activated to initiate protective cellular mechanisms by clearing damaged or dysfunctional mitochondria, maintaining mitochondrial quantity to balance intracellular homeostasis.[24,28] However, the specific molecules and mechanisms through which mitophagy dysfunction in DFU affects wound healing have not yet been fully elucidated.

Combining bioinformatics methods with clinical disease expression profile data is an effective strategy for identifying disease mechanisms, biomarkers, biological pathways, and functions, enabling efficient analysis of large-scale biological datasets. ML, as an artificial intelligence method, utilizes statistical algorithms to analyze datasets and is widely applied in screening feature data from high-throughput data. The integration of bioinformatics and ML algorithms provides a reliable and effective approach for identifying disease-related hub genes. In this study, two mitophagy-related hub genes, ANO6 and ALDH2, were identified through ML methods as being associated with DFU. Both genes were notably downregulated in the DFU group, aligning with the downregulation of ANO6 and ALDH2 observed in clinical skin

https://doi.org/10.2147/JIR.S504001

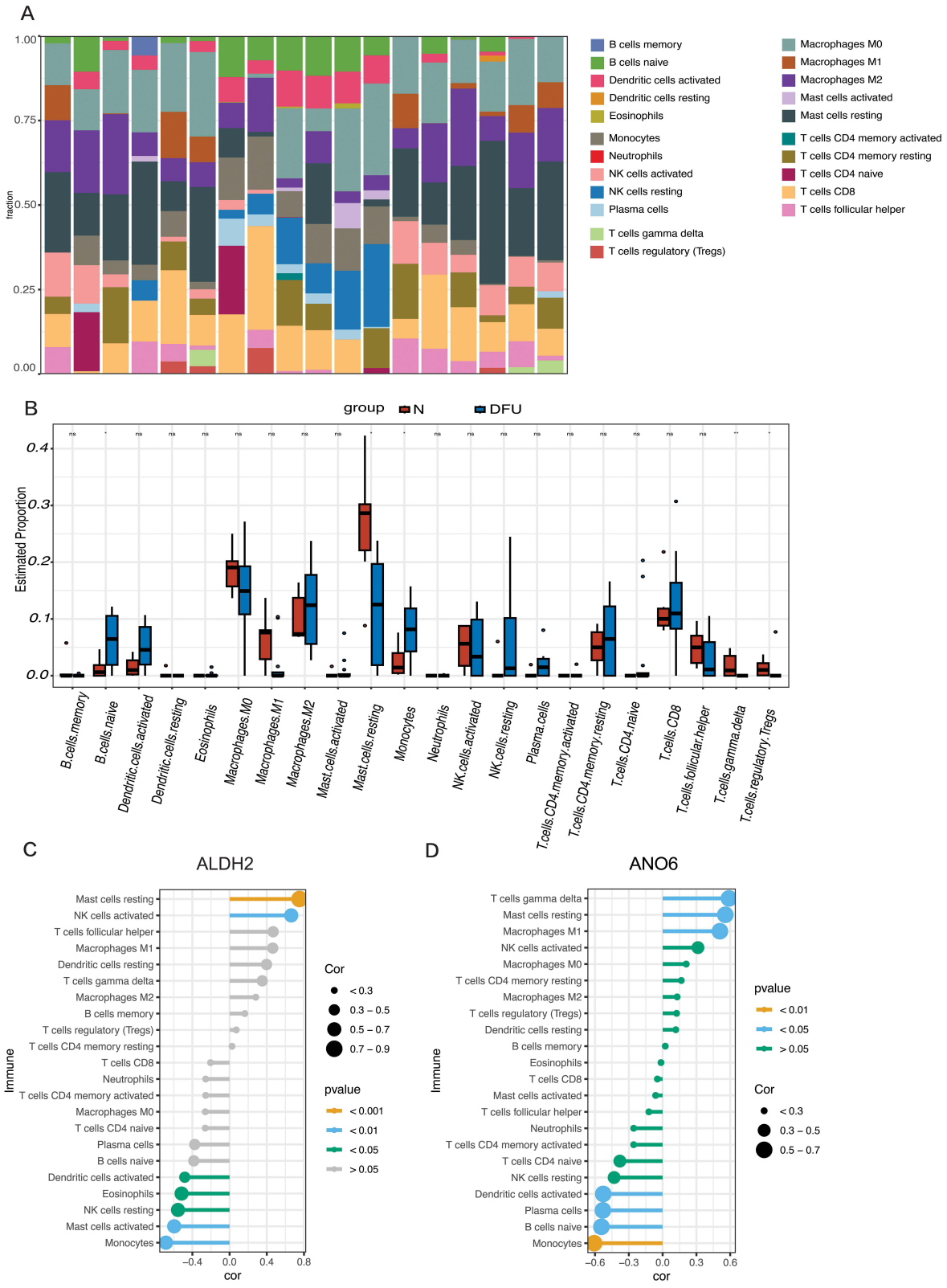

Figure 4 Immune cell infiltration and correlation analysis. (**A**) Relative proportions of 22 immune cell types infiltrating the normal and DFU samples; (**B**) Correlation analysis of immune cell infiltration in the normal and DFU groups, * $p < 0.05$,** $p < 0.01$; (**C** and **D**) Correlation analysis of hub genes with immune cell infiltration.

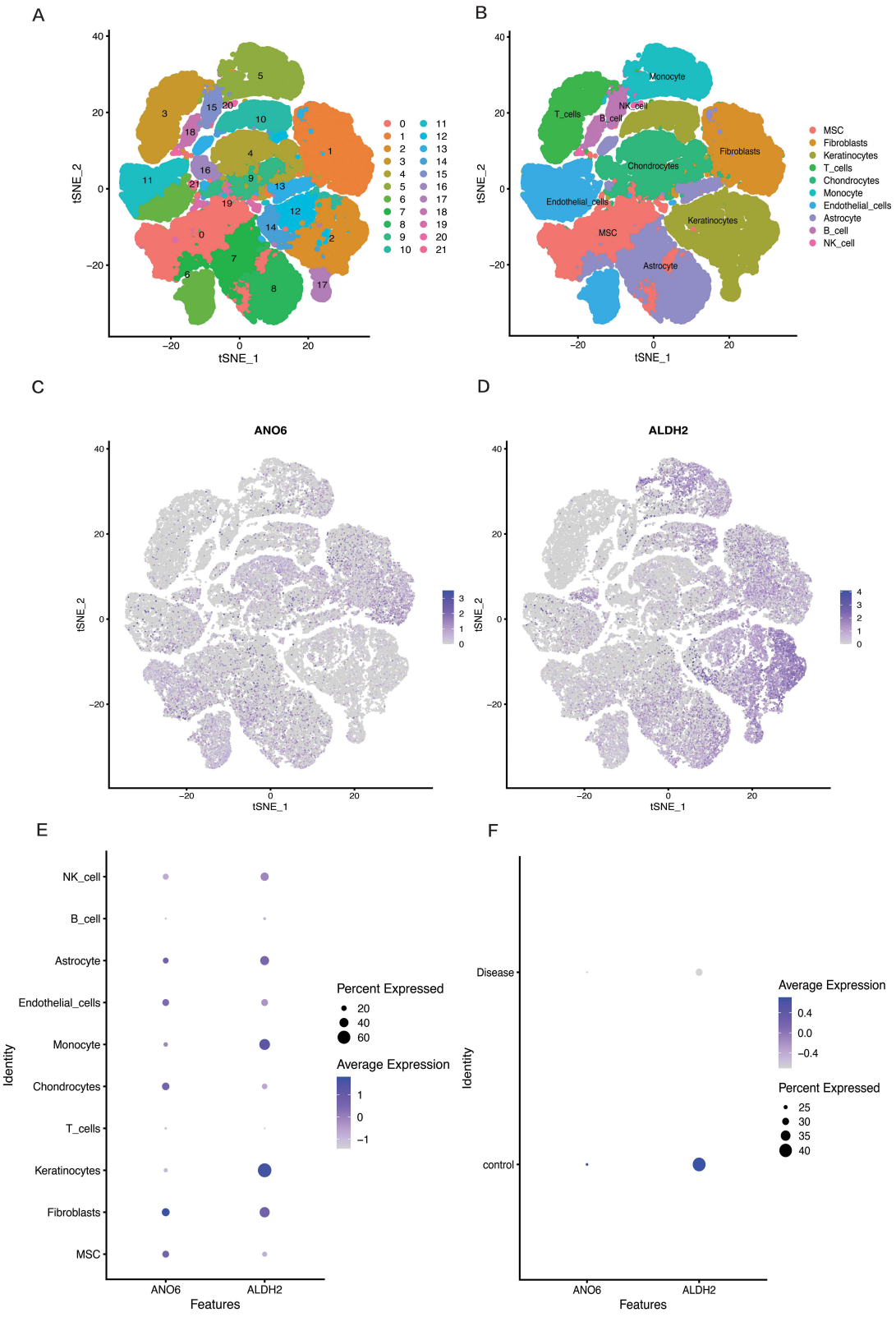

Figure 5 Validation of hub genes at the scRNA-seq level. (**A** and **B**) t-SNE clustering of cells from normal and DFU groups; (**C-E**) Proportions of hub gene expression in various cell types; (**F**) Hub gene expression comparison at the single-cell level between the normal and DFU groups.

https://doi.org/10.2147/JIR.S504001

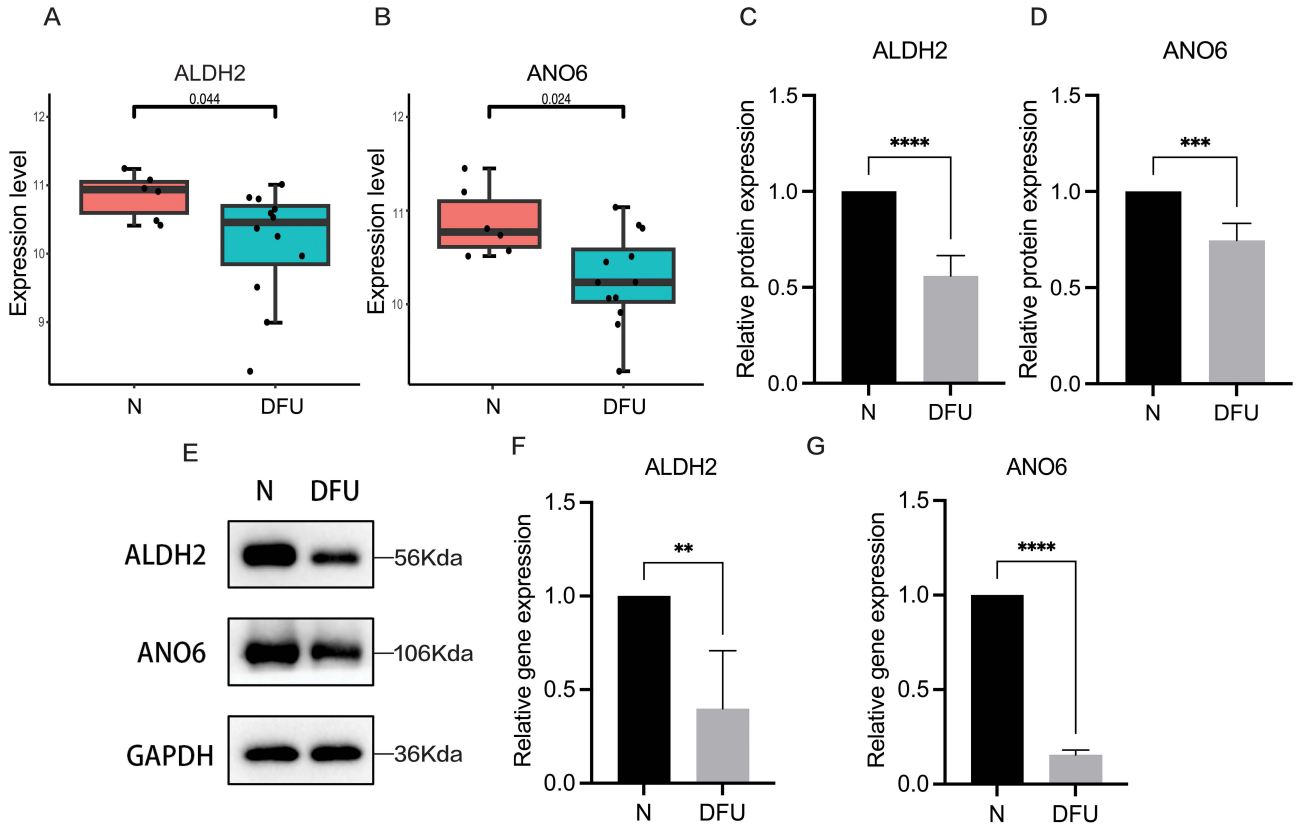

Figure 6 Validation of the expression levels of hub genes in clinical tissues. (**A** and **B**) Hub gene expression comparison in the GSE80178 and GSE68183 datasets between normal and DFU groups; (**C** and **D**) Hub gene RNA expression levels in clinical tissue samples, *** $p < 0.001$, **** $p < 0.0001$; (**E**) Wb assay of hub gene protein expression; (**F** and **G**) Hub gene protein expression levels in clinical tissue samples, ** $p < 0.01$, **** $p < 0.0001$.

tissue samples from DFU patients. This finding revealed that these two hub genes may have a role in the pathogenesis and pathological processes of DFU.

ANO6 encodes a Ca^{2+}-dependent phospholipid scramblase, which mediates the translocation of phosphatidylserine (PtdSer) from the inner leaflet to the outer leaflet of the plasma membrane, increasing the exposure of PtdSer on apoptotic cells, thus releasing signals for macrophage engulfment and promoting the immune system's clearance of apoptotic cells.[29,30] However, ANO6 can cause the externalization of PtdSer in endothelial cells, activating ADAM17 to target and shed the insulin receptor α (IRα), reducing the sensitivity of endothelial cells to insulin and weakening the insulin signaling in the vascular endothelium of diabetic patients.[31–33] ANO6 has also been identified as a Ca^{2+}-activated Cl^- and non-selective cation channel. The increase in Ca^{2+} influx triggers outwardly rectifying Cl^- currents, leading to mitochondrial depolarization and promoting mitochondrial activation.[34] Mitophagy mediated by ANO6 may depend on the biological role of Ca^{2+}, which has long been considered a ubiquitous intracellular second messenger. It plays a crucial role in regulating various biological processes such as development, proliferation, and secretion.[35] The production of ATP within the cell primarily relies on oxidative phosphorylation in the mitochondria, which is regulated by the levels of Ca^{2+} in mitochondrial mechanisms.[36] In macrophages, ANO6 stimulates P2X7R, leading to ATP-induced membrane blebbing and apoptosis, which plays a role in the macrophage-mediated immune response.[37] Ca^{2+} may also alleviate disease-related inflammation by regulating macrophage polarization toward the M1 phenotype.[38] The mechanism by which ANO6 affects DFU remains unclear, in this study, data analysis and experimental results revealed that ANO6 expression was reduced in the skin tissues of DFU patients. Immune infiltration analysis revealed that ANO6 expression was positively correlated with M1 macrophages, suggesting that ANO6 may influence M1 macrophage function and play a role in the pathology of DFU. These findings indicated that ANO6 may affect the pathological state of DFU and

provided a potential target for investigating the molecular mechanisms by which ANO6 regulates the wound healing process in DFU.

ALDH2 is the mitochondrial isoform of aldehyde dehydrogenase. It is responsible for the metabolism of acetaldehyde and other toxic aldehydes.[39] A loss-of-function mutation in ALDH2 is present in 8% of the global population, with about 36% of East Asians (about 560 million) carrying the inactivated Glu504Lys missense mutation in the ALDH2 gene. Large-scale meta-analyses of genome-wide association studies (GWAS) have demonstrated a strong correlation between this inactivating mutation and type 2 diabetes mellitus.[40,41] The accumulation of bioactive aldehydes due to oxidative stress can lead to cell death.[42] For example, 4-hydroxy-2-nonenal (4-HNE), a byproduct of ROS-mediated mitochondrial lipid peroxidation, compromises mitochondrial membrane integrity, inhibits the electron transport chain, and decreases citric acid cycle activity. This reduction in ALDH2 activity increases mitochondrial permeability, induces mitochondrial dysfunction, and ultimately results in DNA damage.[43–45] The lack of ALDH2 promotes the activation of pro-inflammatory macrophages, exacerbating the pathological progression of the disease.[46] In vitro and in vivo experiments that knocked down the ALDH2 gene have confirmed that inhibiting ALDH2 expression can lead to mitochondrial DNA abnormalities, impaired insulin secretion, microvascular organ damage, and disrupted glucose metabolism, ultimately exacerbating the pathological state of diabetes.[47–49] In contrast, the activation of ALDH2 can alleviate inflammation triggered by oxidative stress, promote the elevation of superoxide dismutase (SOD) levels, and inhibit the toxic accumulation of oxidative stress products such as ROS, malondialdehyde (MDA), and 4-hydroxy-2-nonenal (4-HNE) in cells, thereby protecting normal cellular biological functions.[50,51] We observed similar results in this study, with ALDH2 expression being lower in the DFU group relative to the normal group. Previous studies have shown that one of the key reasons for the impaired healing process in DFU is the excessive inflammatory response, which blocks wound healing. Monocytes are integral to the inflammatory response, which differentiate into macrophages to participate in subsequent inflammatory processes. In line with other findings, our immune analysis revealed that ALDH2 expression was inversely correlated with the degree of monocyte infiltration. These results suggested that regulating the ALDH2 gene and protein expression may improve the wound-healing process in DFU.

Certain limitations of our study need to be discussed. Firstly, despite collecting multiple clinical transcriptome databases of typical diseases and using scRNA-seq data for external validation, the relatively small sample size may affect the generalizability and reliability of the study results. Secondly, although this study combines bioinformatics and multiple ML algorithms, along with immune cell infiltration analysis, it still primarily relies on bioinformatics analysis of databases. While clinical tissue samples were collected and used to validate the expression of hub genes to enhance the reliability of the findings, the lack of necessary in vitro and in vivo experimental validation of hub gene functions limits a comprehensive understanding of the identified biomarkers' roles. In addition, the clinical significance of mitophagy-related genes in DFU has not been thoroughly studied. To address these limitations, more extensive datasets and clinical cohort studies are required to validate the robustness of our findings and strengthen the reliability of the identified hub genes as diagnostic markers. Additionally, future research should focus more on the correlation between biological changes and clinical characteristics, which will help develop personalized therapeutic strategies targeting mitophagy. Finally, exploring the efficacy of targeting the identified mitophagy-related hub genes in clinical settings will be crucial for assessing their impact on DFU prognosis. These measures could contribute to establishing a comprehensive genetic framework to support the diagnosis, treatment, and prognosis of DFU.

In conclusion, this study provides new insights into the molecular mechanisms of DFU, with a particular focus on the role of hub genes in DFU and potential therapeutic strategies targeting these genes. Findings from this study provide fresh perspectives on the pathogenesis and genetic mechanisms of DFU, and indicate that ANO6 and ALDH2 may serve as biomarkers for targeted therapy.

Ethics Approval and Informed Consent

The protocol of the present study has received approval by the Ethics Committee, the First Affiliated Hospital of Nanchang University, and adheres to the Declaration of Helsinki. Participants of this study provided written informed consent before the study commenced. Ethics approval number: (2024)CDYFYYLK (08-092).

Author Contributions

All authors made a significant contribution to the work reported, whether that is in the conception, study design, execution, acquisition of data, analysis and interpretation, or in all these areas; took part in drafting, revising or critically reviewing the article; gave final approval of the version to be published; have agreed on the journal to which the article has been submitted; and agree to be accountable for all aspects of the work.

Funding

This work was supported by the National Natural Science Foundation of China (82460447).

Disclosure

The authors report no conflicts of interest in this work.

References

1. Armstrong DG, Tan TW, Boulton AJM, Bus SA. Diabetic foot ulcers: a review. *JAMA*. 2023;330(1):62–75. doi:10.1001/jama.2023.10578
2. Theocharidis G, Thomas BE, Sarkar D, et al. Single cell transcriptomic landscape of diabetic foot ulcers. *Nat Commun*. 2022;13(1):181. doi:10.1038/s41467-021-27801-8
3. Petersen BJ, Linde-Zwirble WT, Tan TW, et al. Higher rates of all-cause mortality and resource utilization during episodes-of-care for diabetic foot ulceration. *Diabet Res Clin Pract*. 2022;184:109182. doi:10.1016/j.diabres.2021.109182
4. Senneville É, Albalawi Z, van Asten SA, et al. IWGDF/IDSA guidelines on the diagnosis and treatment of diabetes-related foot infections (IWGDF/IDSA 2023). *Diabetes Metab Res Rev*. 2024;40(3):e3687. doi:10.1002/dmrr.3687
5. Ä B G, Dorn GW. Evolving and expanding the roles of mitophagy as a homeostatic and pathogenic process. *Physiol Rev*. 99(1):853–892. doi:10.1152/physrev.00005.2018
6. Onishi M, Yamano K, Sato M, Matsuda N, Okamoto K. Molecular mechanisms and physiological functions of mitophagy. *EMBO j*. 2021;40(3):e104705. doi:10.15252/embj.2020104705
7. Kunkemoeller B, Kyriakides TR. Redox signaling in diabetic wound healing regulates extracellular matrix deposition.. *Antioxid Redox Signal*. 2017;27(12):823–838. doi:10.1089/ars.2017.7263
8. Shi TT, Lu HZ, Zhu JY, et al. Naturally derived dual dynamic crosslinked multifunctional hydrogel for diabetic wound healing. *Compos B Eng*. 2023:257110687. doi:10.1016/j.compositesb.2023.110687
9. Li W, Liu X, Liu Z, et al. The signaling pathways of selected traditional Chinese medicine prescriptions and their metabolites in the treatment of diabetic cardiomyopathy: a review. *Front Pharmacol*. 151416403; doi:10.3389/fphar.2024.1416403
10. Liu J, Chen Z, Zhang Y, et al. Rhein protects pancreatic β-cells from dynamin-related protein-1-mediated mitochondrial fission and cell apoptosis under hyperglycemia. *Diabetes*. 2013;62(11):3927–3935. doi:10.2337/db13-0251
11. Chen Y, Liu Q, Meng X, Zhao L, Zheng X, Feng W. Catalpol ameliorates fructose-induced renal inflammation by inhibiting TLR4/MyD88 signaling and uric acid reabsorption. *Eur J Pharmacol*. 967176356. doi:10.1016/j.ejphar.2024.176356
12. Wang M, Yang D, Li L, et al. A Dual Role of mesenchymal stem cell derived small extracellular vesicles on TRPC6 protein and mitochondria to promote diabetic wound healing. *ACS Nano Feb*. 2024;18(6):4871–4885. doi:10.1021/acsnano.3c09814
13. Luo Y, Guo Q, Liu C, Zheng Y, Wang Y, Wang B. Adipose mesenchymal stem cell-derived extracellular vesicles regulate PINK1/parkin-mediated mitophagy to repair high glucose-induced dermal fibroblast senescence and promote wound healing in rats with diabetic foot ulcer. *Acta Diabetol*. 2024. doi:10.1007/s00592-024-02422-x
14. Leal EC, Emanuelli T, Santos D, et al. Dysregulation of endoplasmic reticulum stress response in skin wounds in a streptozotocin-induced diabetes mouse model. *J Mol Endocrinol*. 2023;70(3). doi:10.1530/jme-22-0122
15. Ritchie ME, Phipson B, Wu D, et al. limma powers differential expression analyses for RNA-sequencing and microarray studies. *Nucleic Acids Res*. 2015;43(7):e47. doi:10.1093/nar/gkv007
16. Valero-Mora PM, Huard D, Fonnesbeck CJ. ggplot2: elegant graphics for data analysis. *J Stat Softw*. 2010;35:1–3.
17. Yu G, Wang LG, Han Y, He QY. clusterProfiler: an R package for comparing biological themes among gene clusters. *Omics*. 2012;16(5):284–287. doi:10.1089/omi.2011.0118
18. Yu G, He QY. ReactomePA: an R/Bioconductor package for reactome pathway analysis and visualization. *Mol Biosyst*. 2016;12(2):477–479. doi:10.1039/c5mb00663e
19. Robin X, Turck N, Hainard A, et al. pROC: an open-source package for R and S+ to analyze and compare ROC curves. *BMC Bioinf*. 2011;12:77. doi:10.1186/1471-2105-12-77
20. Hao Y, Stuart T, Kowalski MH, et al. Dictionary learning for integrative, multimodal and scalable single-cell analysis. *Nat Biotechnol*. 2024;42(2):293–304. doi:10.1038/s41587-023-01767-y
21. Wang S, Long H, Hou L, et al. The mitophagy pathway and its implications in human diseases. *Signal Transduct Target Ther*. 2023;8(1):304. doi:10.1038/s41392-023-01503-7
22. Chen W, Zhao H, Li Y. Mitochondrial dynamics in health and disease: mechanisms and potential targets. *Signal Transduct Target Ther*. 2023;8(1):333. doi:10.1038/s41392-023-01547-9
23. Youle RJ, van der Bliek AM. Mitochondrial fission, fusion, and stress. *Science*. 2012;337(6098). doi:10.1126/science.1219855
24. Palikaras K, Lionaki E, Tavernarakis N. Mechanisms of mitophagy in cellular homeostasis, physiology and pathology. *Nat Cell Biol*. 2018;20(9):1013–1022. doi:10.1038/s41556-018-0176-2

25. Galloway CA, Lee H, Nejjar S, et al. Transgenic control of mitochondrial fission induces mitochondrial uncoupling and relieves diabetic oxidative stress. *Diabetes*. 2012;61(8):2093–2104. doi:10.2337/db11-1640
26. Cho JH, Chae CW, Lim JR, et al. Sodium butyrate ameliorates high glucose-suppressed neuronal mitophagy by restoring PRKN expression via inhibiting the RELA-HDAC8 complex. *Autophagy*. 2024;20(7):1505–1522. doi:10.1080/15548627.2024.2323785
27. Cheng X, Huang J, Li H, et al. Quercetin: a promising therapy for diabetic encephalopathy through inhibition of hippocampal ferroptosis. *Article Phytomedicine*. 2024:126154887. doi:10.1016/j.phymed.2023.154887
28. Lazarou M, Sliter DA, Kane LA, et al. The ubiquitin kinase PINK1 recruits autophagy receptors to induce mitophagy. *Nature*. 2015;524 (7565):309–314. doi:10.1038/nature14893
29. Pedemonte N, Galietta LJ. Structure and function of TMEM16 proteins (anoctamins). *Physiol Rev*. 2014;94(2):419–459. doi:10.1152/physrev.00039.2011
30. Le T, Jia Z, Le SC, Zhang Y, Chen J, Yang H. An inner activation gate controls TMEM16F phospholipid scrambling. *Nat Commun*. 2019;10 (1):1846. doi:10.1038/s41467-019-09778-7
31. van Kruchten R, Mattheij NJA, Saunders NJ, et al. Both TMEM16F-dependent and TMEM16F-independent pathways contribute to phosphatidylserine exposure in platelet apoptosis and platelet activation. *Blood*. 2013;121(10):1850–1857. doi:10.1182/blood-2012-09-454314
32. Bevers EM, Williamson PL. Getting to the outer leaflet: physiology of phosphatidylserine exposure at the plasma membrane. *Physiol Rev*. 2016;96 (2):605–645. doi:10.1152/physrev.00020.2015
33. Ferreira-Santos L, Ramirez-Perez FI, Foote CA, et al. Neuraminidase-induced externalization of phosphatidylserine activates ADAM17 and impairs insulin signaling in endothelial cells. *Am J Physiol Heart Circ Physiol*. 326(1):H270–h277. doi:10.1152/ajpheart.00638.2023
34. Suzuki J, Umeda M, Sims PJ, Nagata S. Calcium-dependent phospholipid scrambling by TMEM16F. *Nature*. 2010;468(7325):834–838. doi:10.1038/nature09583
35. East DA, Campanella M. Ca 2+ in quality control. *Autophagy*. 2013;9(11):1710–1719. doi:10.4161/auto.25367
36. Boyman L, Karbowski M, Lederer WJ. Regulation of mitochondrial ATP production: ca(2+) signaling and quality control. *Trends Mol Med*. 2020;26(1):21–39. doi:10.1016/j.molmed.2019.10.007
37. Ousingsawat J, Wanitchakool P, Kmit A, et al. Anoctamin 6 mediates effects essential for innate immunity downstream of P2X7 receptors in macrophages. *Nat Commun*. 2015;6:6245. doi:10.1038/ncomms7245
38. Lv Z, Xu X, Sun Z, et al. TRPV1 alleviates osteoarthritis by inhibiting M1 macrophage polarization via Ca(2+)/CaMKII/Nrf2 signaling pathway. *Cell Death Dis*. 2021;12(6):504. doi:10.1038/s41419-021-03792-8
39. Chen CH, Ferreira JC, Gross ER, Mochly-Rosen D. Targeting aldehyde dehydrogenase 2: new therapeutic opportunities. *Physiol Rev*. 2014;94 (1):1–34. doi:10.1152/physrev.00017.2013
40. Chang YC, Lee HL, Yang W, et al. A common East-Asian ALDH2 mutation causes metabolic disorders and the therapeutic effect of ALDH2 activators. *Nat Commun*. 2023;14(1):5971. doi:10.1038/s41467-023-41570-6
41. Spracklen CN, Horikoshi M, Kim YJ, et al. Identification of type 2 diabetes loci in 433,540 East Asian individuals. *Nature*. 2020;582 (7811):240–245. doi:10.1038/s41586-020-2263-3
42. Liang J, He YW, Huang CX, Ji FJ, Zhou XH, Yin YL. The regulation of selenoproteins in diabetes: a new way to treat diabetes. *Curr. Pharm. Des*. 2024;30(20):1541–1547. doi:10.2174/0113816128302667240422110226
43. Chen CH, Sun L, Mochly-Rosen D. Mitochondrial aldehyde dehydrogenase and cardiac diseases. *Cardiovasc Res*. 2010;88(1):51–57. doi:10.1093/cvr/cvq192
44. Ma H, Guo R, Yu L, Zhang Y, Ren J. Aldehyde dehydrogenase 2 (ALDH2) rescues myocardial ischaemia/reperfusion injury: role of autophagy paradox and toxic aldehyde. *Eur Heart J*. 2011;32(8):1025–1038. doi:10.1093/eurheartj/ehq253
45. Sun X, Gao R, Li W, et al. Alda-1 treatment promotes the therapeutic effect of mitochondrial transplantation for myocardial ischemia-reperfusion injury. *Bioact Mater*. 2021;6(7):2058–2069. doi:10.1016/j.bioactmat.2020.12.024
46. Rui H, Yu H, Chi K, et al. ALDH2 deficiency augments atherosclerosis through the USP14-cGAS-dependent polarization of proinflammatory macrophages. *Redox Biol*. 2024;76:103318. doi:10.1016/j.redox.2024.103318
47. Tan X, Chen YF, Zou SY, et al. ALDH2 attenuates ischemia and reperfusion injury through regulation of mitochondrial fusion and fission by PI3K/AKT/mTOR pathway in diabetic cardiomyopathy. *Free Radic Biol Med*. 2023;195:219–230. doi:10.1016/j.freeradbiomed.2022.12.097
48. Suzuki Y, Muramatsu T, Taniyama M, et al. Mitochondrial aldehyde dehydrogenase in diabetes associated with mitochondrial tRNA(Leu(UUR)) mutation at position 3243. *Diabetes Care*. 1996;19(12):1423–1425. doi:10.2337/diacare.19.12.1423
49. Wohlfart DP, Lou B, Middel CS, et al. Accumulation of acetaldehyde in aldh2.1(-/-) zebrafish causes increased retinal angiogenesis and impaired glucose metabolism. *Redox Biol*. 2022;50:102249. doi:10.1016/j.redox.2022.102249
50. Knopp RC, Lee SH, Hollas M, et al. Interaction of oxidative stress and neurotrauma in ALDH2(-/-) mice causes significant and persistent behavioral and pro-inflammatory effects in a tractable model of mild traumatic brain injury. *Redox Biol*. 2020;32:101486. doi:10.1016/j.redox.2020.101486
51. Kang P, Wang J, Fang D, et al. Activation of ALDH2 attenuates high glucose induced rat cardiomyocyte fibrosis and necroptosis. *Free Radic Biol Med*. 2020;146:198–210. doi:10.1016/j.freeradbiomed.2019.10.416